Medical Engineering and Physics 119 (2023) 104027

Contents lists available at ScienceDirect

Medical Engineering and Physics

journal homepage: www.elsevier.com/locate/medengphy

Technical note

Micromotion measurement at the interfaces of cemented tibial endoprosthetic replacements: A new standardized in vitro model using open-cell rigid foam

Christian Fölsch [a,b,*], Carlos Alfonso Fonseca Ulloa [b], Torben Harz [b], Julia Schirmer [b], Cosmin Glameanu [a,b], Jan Scherberich [c], Gabriele Krombach [c], Markus Rickert [a,b], John Ryan Martin [d], Klaus-Dieter Kühn [e], Alexander Jahnke [b]

[a] Department of Orthopaedics and Orthopaedic Surgery, University Hospital Gießen and Marburg (UKGM), Justus-Liebig-University, Klinikstraße 33, 35392 Gießen, Germany
[b] Laboratory of Biomechanics, Justus-Liebig-University Gießen, Klinikstraße 29, 35392 Gießen, Germany
[c] Department of Diagnostic and Interventional Radiology, Laboratory for Experimental Radiology, Justus-Liebig-University, Klinikstraße 33, 35392 Gießen, Germany
[d] Vanderbilt University Medical Center, 1215 21st Ave S Suite 4200, Nashville, TN 37232, USA
[e] Department of Orthopaedics and Orthopaedic Surgery, Medical University Graz, Auenbruggerstraße 5, Graz, Austria

ARTICLE INFO

Keywords:
Loosening knee arthroplasty
Micromotion
Interface cement-bone and implant-cement
Open-cell rigid foam
Cementation technique

ABSTRACT

Early aseptic loosening following primary total knee arthroplasty related to several factors might appear at the interface implant-cement or cement-bone. A standardized in vitro model might provide information on the relevance of single variable parameter of cementation including technique and cement respectively bone structure on fixation strength. Micromotion measurement using different directions of load should detect the primary stability of the interfaces.

An open-cell rigid foam model was used for cementation of PFC-Sigma tibial trays with Palacos®. Pins were applied to the model for continuous non-destructive measurement. Relative micromotions for rotation, valgus-varus and extension flexion stress were detected at the interfaces as well as cement penetration was measured.

The reproducibility of the measurement could be shown for all interfaces in extension-flexion movements. For rotation a negative trend was shown for the interface cement-prosthesis and cement-bone concerning varus-valgus stress reflecting varying surgical cementation technique. More micromotion related to extension-flexion force might reflect the design of the implant.

Measurement of relative micromotion and cement distribution appear accurate to detect small differences of movement at different interfaces of cemented tibial implants and the results are reproducible for most parameter. An increased number of specimens should achieve statistical relevance for all measurements.

1. Introduction

Fixation of joint replacements is essential for good long term results of arthroplasties and among other factors the cementing technique is crucial to prevent early failure [1]. An in vitro model seems useful to study multiple factors influencing the stability at the interfaces implant-cement and cement-bone. Human cadaver bone is expensive and interindividual variation of bone structure should be considered. The three-dimensional structure of open-cell sawbone resembles human cancellous bone and different densities corresponding to natural variation of bone structure are available [2,3]. The trabecular thickness and bone volume fraction of open-cell rigid foam is comparable to human cancellous bone since the main diameter of the cavities varies negligible [4]. Synthetic foams simulate elastic properties of cancellous bone and related to different shear strength behavior non-destructive tests should preferred since the mechanic behavior under compression appears similar [2,5]. Open-cell foam resembles fracture behavior of human cancellous bone better than solid sawbone [6,7].

Standardized properties of the synthetic foam were developed and the cell size is not specified (ASTM F1839) [2]. We used open-cell foam

* Corresponding author at: Department of Orthopaedic Surgery, Justus-Liebig-University, Klinikstraße 33, 35392 Gießen, Germany.
E-mail addresses: christian.foelsch@t-online.de, christian.foelsch@ortho.med.uni-giessen.de (C. Fölsch).

https://doi.org/10.1016/j.medengphy.2023.104027
Received 4 February 2023; Received in revised form 31 May 2023; Accepted 19 July 2023
Available online 20 July 2023

with a medium density since higher density reduced open-cell porosity [4]. Measurement of primary stability of implant fixation immediate after cementation is possible in vitro. Measurement of micromotion allows a non-destructive examination of the interface cement implant and cement bone (ASTM F2537-06) allowing a more precise analysis of the mode of failure. Therefore, we measured micromotion at the interfaces implant to cement and cement to bone related to multidirectional loading. Micromotion was influenced by density and direction of load [8]. Pull-out test of tibial trays do not simulate the mechanic load in vivo and therefore the meaningfulness for clinical implications seems limited [9,10]. Torsional tests until failure do not measure forces at different sites of the implant since only the weakest interface fails [11].

The open-cell structure of the foam allows a distribution of cement comparable with the interconnectivity of human cancellous bone. To date there is no suitable open-cell artificial bone model for investigation of cemented tibial implants. This is the first study applying an open-cell rigid foam model for measurement of micromotion regarding the stability of cemented tibial trays. An inexpensive standardized in vitro tibial bone model should be established to test the influence of multiple factors on the strength of the fixation of implants at different sites. This might provide further information for improvement of cementation technique and implant design.

2. Methods

2.1. Tibial endoprosthesis

The tibial component size 1.5 of P.F.C Sigma® fixed bearing endoprosthesis (DePuy Synthes, Warsaw, IN, USA) was used. The prosthesis is coated with a titanium alloy (Ti6Al4V) and is to be anchored with cement only. Using a 1.9 mm solid carbide high-performance drill (TiAlNplus, Atorn®, Hahn+Kolb Werkzeuge GmbH, Ludwigsburg, Germany) a hole was drilled 2 mm below the upper edge of the prosthesis in the center of the ventral and lateral side of the plateau for attachment of measuring pins. An M8 thread was cut into the recess in the prosthesis intended for the inlay. This thread was used for later attachment of the measuring lever applying the force loading into the prosthesis.

2.2. Synthetic bone material

Material parameters of human cancellous bone show a very large variance [12,13]. Therefore we used an artificial bone model of open-cell rigid foam bone material with a density of 20 PCF (Sawbones Europe AB, Malmö, Sweden) which was developed according to the geometry of the implant. This material corresponds to a density of 0.32 g/cm^3, a porosity of 0.21, a compression strength of 1.3 MPa, and a Young's modulus of 105 MPa. Sawbone shows a standardized and relatively low modulus of elasticity, but has similar properties to the trabecular hip bone, taking into account the localization of the cancellous bone tissue(bone density: 0.35 g/cm^3; porosity: 0.69 ± 0.1; Young's modulus: 116.4 ± 86.7 MPa) [6,14]. Available blocks measure 130 mm x 180 mm x 40 mm and individual blocks with the dimensions 40 mm (anterior – posterior direction) x 60 mm (medial – lateral direction) x 65 mm (cranial – caudal direction) were cut with a circular saw.

The tibial plateau was milled into the bone foam using the milling attachment of a 3D printer (Snapmaker 2.0, A350T, Snapmaker, Shenzhen, China). To simulate the cortical bone and to prevent cement flowing out of the bone, a synthetic support bandage (Cellacast® Xtra, Lohmann & Rauscher International GmbH & Co. KG, Rengsdorf, Germany) size 5 cm x 3.6 m was used. To ensure a good bond between the cast and the bone foam, epoxy resin E45 was mixed with hardener E45 (Martin Pauck Company, Hamburg, Germany) in a 1:1 ratio and applied thinly to the bone foam using a brush before applying the cast. The Cellacast® was then immersed in 20 °C water and wrapped around the bone foam six times and pressing continuously. The protruding edges of the cast were ground off creating a flat surface on the tibial plateau (Fig. 1).

Before implantation the tibial plateau model was clamped in a specially made centering aid to ensure the implantation template is congruent with the model. The guide was attached to the model as closely as possible to ensure reproducibility and axis-correct medullary canal preparation. The medullary reamer was then used to drill into the plateau up to the specified mark on the drilling attachment. The rasp was hammered into the tibial plateau model using the guide device and the medullary canal was finally prepared (Fig. 2).

The tibial plateau model was then fixed vertically in plaster. Exact horizontal and vertical alignment was performed using a self-leveling line laser (Quigo, Bosch, Leinfelden-Echterdingen, Germany) in two planes (sagittal and transversal) and from two sides (ventral and lateral).

2.3. Bone cement

Palacos® R Bone Cement (Heraeus Medical GmbH, Wehrheim, Germany) was used. One ampoule (20 ml) of the monomer liquid component was first poured into the mixing vessel before the whole bag (40 g) of the polymer powder component was added (start of timing) and mixed under vacuum for 30 s with the vacuum mixing system Palamix® (Heraeus Medical GmbH, Wehrheim, Germany). The room temperature was kept constant at 19 ± 1 °C during cementation.

2.4. Cementation of implant

The Inspekt table blue 20 kN materials testing machine (Hegewald & Peschke GmbH, Nossen, Germany) was used to implant the prosthesis. The prosthesis was aligned congruently in the tibia plateau model in advance and then raised 60 mm proximally with the machine. After 1.5 min the mixed cement was retrogradely applied by an experienced surgeon into the medullary canal with a cement gun and by hand to the underside of the prosthetic plateau and to the stem of the prosthesis. The entire cement quantity was used in each case to standardize the amount of cement applied. After 3.0 min the implant was guided away to a distance of 0.1 mm from the tibial plateau with a constant feed speed of 300 mm/min recording the implantation force.

2.5. Computertomographic examination

Computertomographic examination of the models was performed following hardening of the cement (Siemens Somatom Force). The slice thickness of the tomograph was 0.3 mm. The digital models were evaluated with dataviewer (Data Viewer V. 1.5.6.2, Bruker microCT, Billerica MA, USA). The prosthesis was digitally extracted and the models were evaluated axially and sagittally. After manually choosing of an area of interest being equal in size to the bone in the first scan layer the scans were binarized. The cement with the foam or high-density elements was represented in the image as white and the air was represented in the image as black. After the binarization of the models several metrics were evaluated: total volume of all binarized elements was calculated (Obj.V), percentage of elements with higher density (white) in relation to the whole object (Obj.V/TV) were computed and the total surface area of all connected voxels with higher density were measured using the marching cubes' method (Obj.S). The average of all 2D surfaces of the higher-density connected voxels was also calculated (Obj.Pm). The ratio of the 3D volumes of air, which are completely enclosed within the higher-density structures, to the total volume of the higher-density elements was computed over the entire region of interest (Po(cl)).

To measure the cement penetration into different osseous structures, the raw images were used and the objects were divided into three regions of interest: anterior-medial, anterior-lateral and posterior. With the software Infinity the middle of the prosthesis was located considering the dorsal flange of the prosthesis. Once the middle of the

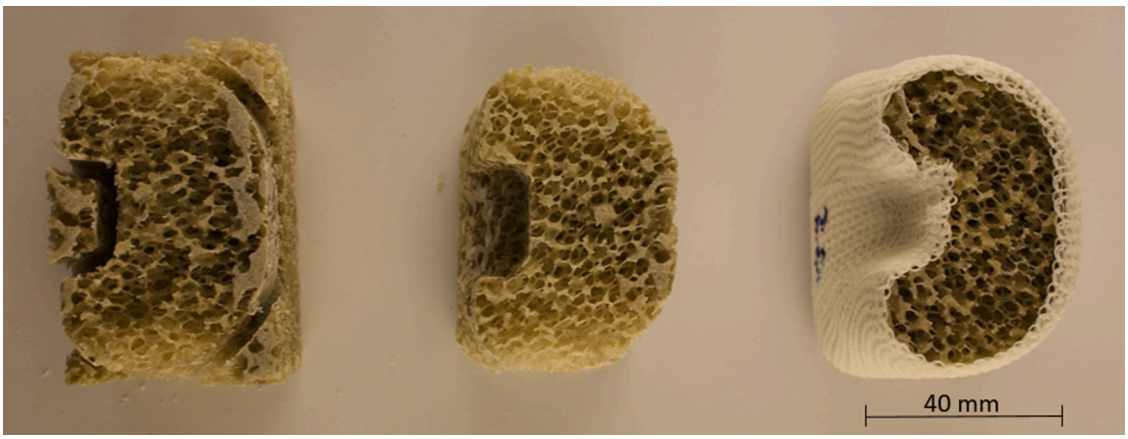

Fig. 1. Left: Milled model with protruding edges. Middle: Model with broken edges. Right: Model with wrapped Cellacast® as cortical bone.

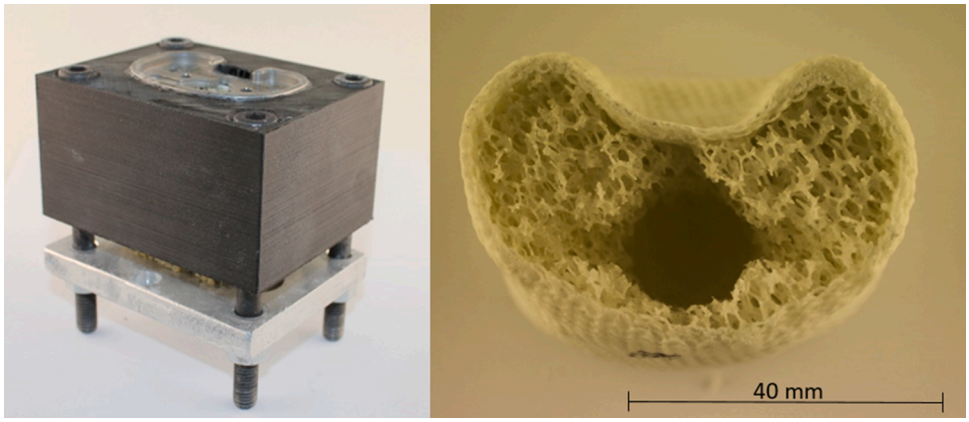

Fig. 2. Left: Fixation of the model in custom-made 3D-printed orientation aid and integrated centering device. Right: Medullary canal preparation with manufacturer-specific surgical instruments.

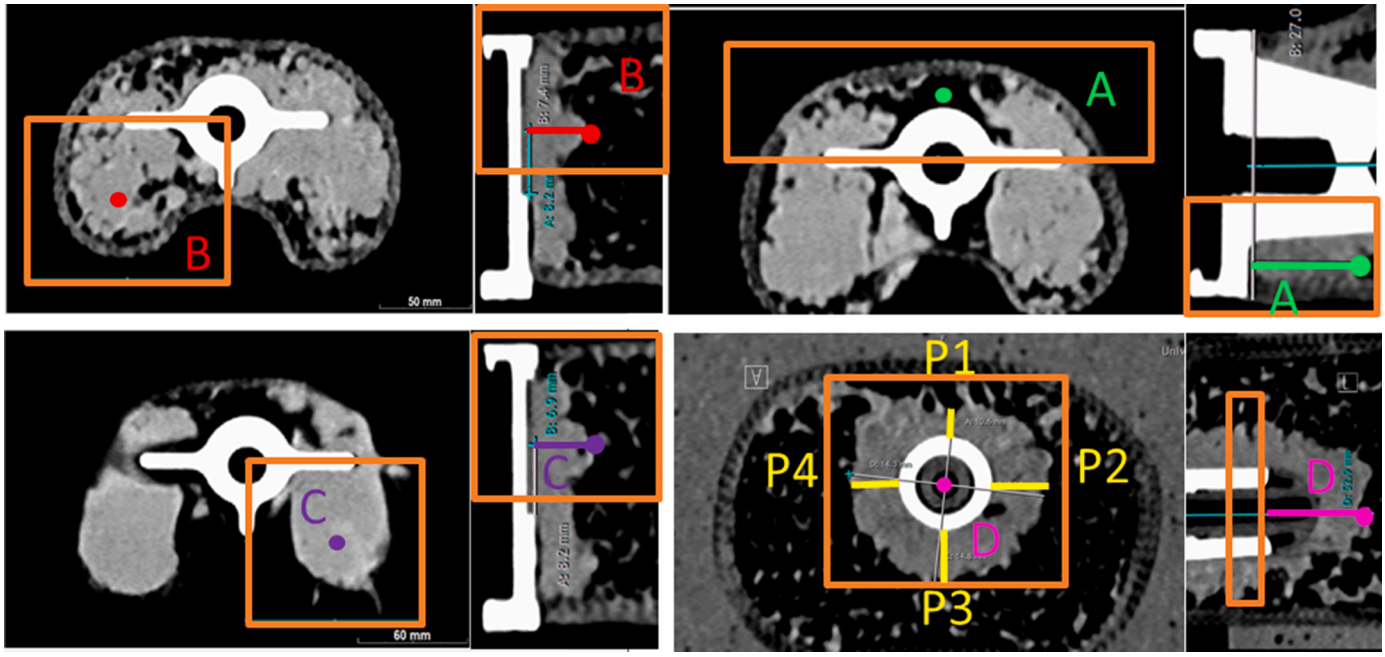

Fig. 3. Representation of the computertomographic examined areas and representation of the measuring points of the cement penetration.

prosthesis was found, 4 mm were measured from the posterior part of the bone in a dorsal direction. From this point and in the caudal direction, the frontal penetration of the cement (A) was measured. Also, from the middle of the prosthesis, but starting in the middle of the prosthesis stem, the maximal distal penetration was measured caudally (D). Following the geometry of the prosthesis, two other points were determined, one lateral anterior and another medial anterior. To define these points the sagittal images were used and thanks to the lateral and medial flanges of the prosthesis the indicated scan-layer was found to measure the penetration in these regions. Taking the cement bone surface as a start position of measurement two points were determined in the middle of the images. From these points the lateral and medial penetration of the cement into the bone was established (B and C).

For the measurement of the distally penetration of the prosthesis around the stem the axial sequence of the scanner was used. The measurement point was defined as the last scan-layer with the prosthetic stem being completely visible and forming a perfect circle. From this point and considering the bone axis the cement penetration was measured in all directions (anterior (P1), lateral (P2), medial (P3), and dorsal (P4)) (Fig. 3).

2.6. Primary stability analysis

After CT radiological measurement primary stability analysis was performed. Running parameters taken from Orthoload.com at 4 km/h were taken as basis. 10% of the maximum torque measured during running was used to apply torques at the prosthesis (3.5 Nm). This ensures that motion of the prosthesis-cement-bone composite is in a non-destructive range and large enough to measure micromotion. Measuring pins were attached to the prosthesis-cement-bone composite. For the cortical bone measurement points (B_1/B_2), this was done by drilling 4 mm deep into the Cellacast® with a 1.8 mm drill on the dorsal and medial sides and 5 mm below the lower edge of the prosthesis. To prepare the cement measuring points (C_1/C_2), the Cellacast® was drilled on the ventral and lateral side, 5 mm below the lower edge of the prosthesis with a 5.8 mm drill and then drilled 4 mm deep into the cement with the 1.8 mm drill. The measuring pins were then attached to the measuring points of the prosthesis (P_1/P_2), the cortical bone (B_1/B_2) and the cement (C_1/C_2) using super glue.

Using an already established non-contact eddy current measurement system [15,16] (type NCDT 3010-S2, Micro-Epsilon Messtechnik GmbH & Co. KG, Ortenburg, Germany) the relative micromotions of the prosthesis, the cement and the bone were detected with a resolution of 0.1 μm (Fig. 4). For this purpose, the measuring pins were connected one after the other to an orthogonally aligned aluminum cube. The eddy current sensors enclosed in a measuring frame were attached to the lever arm adapter by means of a tripod arm. This point is the reference point. Subsequently, reaction-free torques about the Z-axis as well as tilting torques in ventro-dorsal (extension and flexion loading) and medio-lateral (varus-valgus loading) directions were introduced into the prosthesis-cement-bone bond via the lever arm.

2.7. Evaluation of relative micromotion

The acquired relative micromotions were evaluated using a MATLAB-program (version 2020b, The MathWorks, Inc., Natick, MA, USA) to map the rotation vectors $\Omega\rightarrow$ in the form of a hysteresis curve whose slope corresponds to the normalized rotation angle α in mdeg/Nm. Taking into account the corresponding radii and distances of the individual measurement objects from each other, the normalized relative interface movement between implant, cement mantle and bone can also be calculated in μm/Nm. This could then be used to approximate the absolute interface movement taking into account actual in vivo loads [15,16]. This mathematical procedure is not relevant for the evaluation of this model with regard to its reproducibility.

2.8. Statistics

To validate this model and our method one prosthesis was repeatedly measured five times. After non-destructive testing, the implant was always removed from the bone model without damage using an acetone bath before implantation into a new bone model was done. Implantation force, relative micromovements and computertomographic parameters, in particular the cement penetration, were subsequently analyzed for repeatability using SPSS 29.0 (SPSS Inc., IBM, Chicago, USA). For this purpose, the Jonckheere-Terpstra trend test was used to investigate whether repeatable results could be obtained with this model. Possible correlations between the parameters were analyzed using the Kendall-Tau test. A p-level < 0.05 was considered statistically significant.

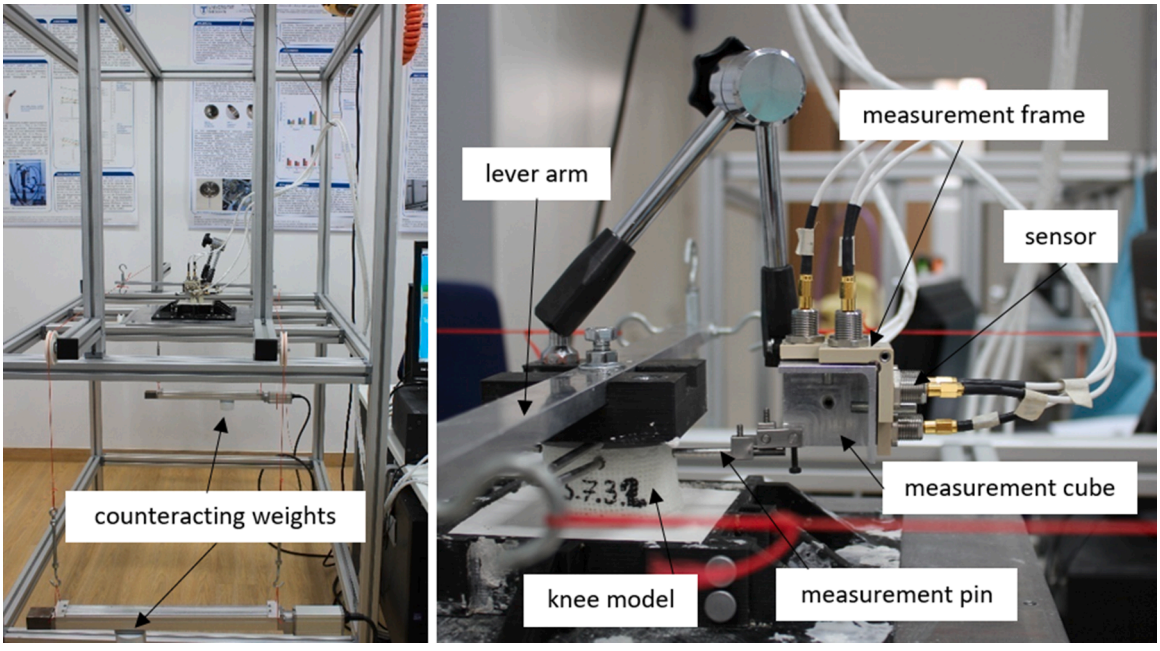

Fig. 4. Left: The measuring device. Right: The measuring setup more detailed.

3. Results

3.1. Mechanical parameters

The following table shows the repeated measurements of the implantation forces as well as the data of the primary stability analysis. Statistical analysis revealed a strong negative trend ($p = 0.05$; $\tau = -0.8$) with repeated measurement for the rotational movement around the Z-axis between the cement and the prosthesis. The varus-valgus movement between the cement and bone also showed a strong negative trend ($p < 0.05$; $\tau = -0.8$) with repeated measurement (Table 1).

3.2. Radiology results

Table 2 shows the different parameters of the radiological analysis, which represents the properties of the cement mantle within the bone model. Only the porosity of the cement showed a strong negative trend with repeated measurement ($p < 0.05$; $\tau = -0.8$).

The measurement results of the cement penetration depth at the different measuring points did not identify any trends (Table 3).

4. Discussion

Measurement of pull-out force has been used for mechanical testing of the interface of tibial implant and cement [9,10,17,18] as well as cement and bone since torsion and compression have also been applied [11,19]. The mode of measurement was either until failure of the implant or micromotion was detected using mechanic or optical techniques [19,20,21]. Micromotion at different locations following cyclic loading of tibial trays in cadaveric bone measured with digital image correlation had shown deviating results [22,23]. A high resolution camera system detected different micromotion at the interface cement and bone related to different areas in postmortal tibiae [23,24]. The direction of load should resemble the forces expected in vivo and therefore torsion and valgus-varus stress as well as extension and flexion seem appropriate. We used 0.32 g/cm^3 open-cell sawbone resembling average bone quality and fracture behavior of human cancellous bone [7]. The average pore size of sawbone ranged from 125 µm to 234 µm for densities between 0.641 g/ cm^3 and 0.159 g/ cm^3 [2].

Micromotion was a sensitive parameter to detect torsion differences related to the design of knee-replacements [8,19,20] and demonstrated an increase of stability for cementing tibial tray stems [21]. Deviations of micromotion at different sites of the implant could be detected [19]. Measurement of micromotion could differentiate fixed from unstable implants since multiple factors influenced the fixation [8]. An in vitro model should be useful to examine the effect of these factors since the range of measurements for stable and loose implants is overlapping. Different fixation techniques of tibial trays mainly related to cementation revealed deviating results for micromotion [8,25,26]. Therefore, that method appears useful to study the effect of different implant designs and cementing techniques on implant fixation (ASTM F2537-06) [8,19,21,25,26].

Table 2
Presentation of cement properties based on various radiology parameters. Parameters that showed a significant trend are highlighted in gray.

Cement distribution					
ID	Obj.V [mm^3]	Obj.V/TV [%]	Obj.S [mm^2]	Obj.Pm [mm]	Po(cl)%). [%]
#1	278,923.4	58.5	136,601.4	814.6	20.6
#2	276,970.5	58.8	115,229.2	714.0	22.1
#3	335,149.0	65.1	120,748.1	729.1	19.0
#4	343,272.4	63.4	130,248.1	782.8	18.6
#5	307,265.8	61.7	132,637.7	718.6	18.2
MEAN	**308,316.2**	**61.5**	**127,092.9**	**751.8**	**19.7**
SD	**30,779.6**	**2.9**	**8833.4**	**44.6**	**1.6**

Measurement of micromotion could detect more motion for cementless than for cemented tibial trays [27,28]. Micromotion might show different results for interfaces implant and cement within a range being defined as clinical stable [23]. Loosening was diagnosed with a motion of 110 µm and in vitro an interdigitation between cement and bone allowing less than 1 µm motion could be achieved [23]. Improvement of initial fixation between implant and cement as well as cement and bone might prolong the longevity of the fixation. Micromotion was correlated with interdigitation of cement and bone [23]. Interdigitation of cement and bone diminishes with time [23,24] and cement degrades [28,29]. Postmortem studies showed a loss of 75% cement-bone interlock within 10 years [24] pointing out the relevance of best primary intraoperative fixation.

Only rotational movement around the central axis and the varus and valgus loading in the implant-cement interface showed a negative trend (Table 1) also being shown for porosity related to air enclosed in the cement (Table 2). The impaired reproducibility for that 3 parameter suggests an influence of the surgical procedure. The vast majority of variables showed reproducibility of the measurement and this appeared excellent for the cement distribution (Tables 2, 3). We attribute the emergence of trends of $n = 3$ out of a total of $n = 24$ considered variables to the small number of cases of $n = 5$ since a coincidence with the large number of parameters has to be considered.

Some limitations are naturally related to an in vitro model since synthetic bone structures cannot reflect the complex morphology and material properties of human bone. Artificial bone provides more reproducible and standardized conditions since comparison of results is simplified and changing single variables is possible in vitro. Clinical transfer should be considered carefully.

5. Conclusions

This is the first in vitro model allowing physiologic cement distribution due to the open-cell structure of the synthetic bone allowing better comparison with in vivo situation combined with measurement of relative micromotion. The open-cell rigid foam model allows reproducible and accurate measurements of relative micromotions between

Table 1
Repeated measurements of the implantation force and the relative micromotions between the different interfaces considering several loading directions. Parameters that showed a significant trend are highlighted in gray.

Mechanical parameters										
		Rotation (Z-Axis) [mdeg/Nm]			Varus-Valgus (X-Axis) [mdeg/Nm]			Extension-Flexion (Y-Axis) [mdeg/Nm]		
ID	Implantation force [N]	Cement-prosthesis	Cement-bone	Prosthesis-bone	Cement-prosthesis	Cement-bone	Prosthesis-bone	Cement-prosthesis	Cement-bone	Prosthesis-bone
#1	120.2	3.9	2.6	1.3	2.4	3.7	1.1	1.2	23.1	33.6
#2	152.3	7.4	0.1	7.6	5.9	7.2	1.4	1.5	8.6	7.1
#3	115.8	3.3	2.7	0.6	4.4	2.8	1.6	1.0	21.8	20.9
#4	80.4	2.4	4.2	6.6	3.1	1.7	4.8	0.2	9.9	9.7
#5	111.9	1.0	2.6	3.6	0.8	0.1	0.9	1.0	27.5	26.6
MEAN	**116.1**	**3.6**	**2.4**	**3.9**	**3.3**	**3.1**	**2.0**	**1.0**	**18.2**	**19.6**
SD	**25.6**	**2.4**	**1.5**	**3.1**	**1.9**	**2.7**	**1.6**	**0.5**	**8.4**	**11.2**

Table 3
Presentation of the measurement results of the cement penetration depth.

Cement penetration								
	Plateau				Stem			
ID	Anterior	Lateral	Medial	Distal	Anterior (P1)	Lateral (P2)	Dorsal (P3)	Medial (P4)
#1	4.7	7.4	6.9	4.4	10.8	13.4	16.6	14.0
#2	13.7	8.2	9.7	3.8	13.3	10.4	14.9	14.2
#3	13.3	4.7	5.5	6.5	16.1	14.0	13.6	16.6
#4	12.9	8.7	7.2	7.6	10.6	14.5	14.8	14.3
#5	14.0	6.1	6.8	3.6	14.3	13.1	14.2	16.4
MEAN	**11.7**	7.0	**7.2**	**5.2**	**13.0**	**13.1**	**14.8**	**15.1**
SD	**3.9**	**1.6**	**1.5**	**1.8**	**2.3**	**1.6**	**1.1**	**1.3**

tibial implant and cement as well as between cement and bone. This model can be used to study the influence of different factors on cementation of tibial components of knee endoprostheses nearly resembling the in vivo situation. Different density foam might resemble structural changes of the bone structure. The complex interactions of factors influencing the final quality of fixing the implant favor an inexpensive und highly reproducible accurate model to examine changeable factors. The detection of varying loads at different sites of the tibia implant and the range of micromotions related to directions of load emphasizes further potential of the new model. A more homogenous distribution of cement might contribute to smaller differences of micromotions below the implant. This in vitro model should give relevant information to improve the interdigitation between cement and implant which could optimize cementation techniques. Further improvement of the primary stability of fixation of cemented tibia implants of knee joint replacements seems important to prolong the longevity of the implants.

Funding

None.

Ethical approval

Not required

CRediT authorship contribution statement

Christian Fölsch: Resources, Conceptualization, Methodology, Formal analysis, Funding acquisition, Project administration, Writing – original draft, Writing – review & editing. **Carlos Alfonso Fonseca Ulloa:** Software, Supervision, Data curation. **Torben Harz:** Software, Data curation, Supervision. **Julia Schirmer:** Investigation. **Cosmin Glameanu:** Investigation. **Jan Scherberich:** Visualization, Validation, Software. **Gabriele Krombach:** Data curation, Validation. **Markus Rickert:** Supervision, Writing – review & editing. **John Ryan Martin:** Resources, Conceptualization. **Klaus-Dieter Kühn:** Conceptualization, Resources, Supervision. **Alexander Jahnke:** Methodology, Conceptualization, Supervision, Formal analysis, Writing – original draft.

Declaration of Competing Interest

There are no conflicts of interest to declare.

Acknowledgements

This study was kindly funded by Heraeus Medical LLC, 770 Township Line Road, Yardley PA 19067, United States of America.

References

[1] Martin JR, Otero JE, Mason JB, Fehring TK. Where is the "Weak Link" of fixation in contemporary cemented total knee replacements? J Arthroplasty 2021;36(7):2497–501.
[2] Calvert KL, Trumble KP, Webster TJ, Kirkpatrick LA. Characterization of commercial rigid polyurethane foams used as bone analogs for implant testing. J Mater Sci: Mater Med 2010;21:1453–61.
[3] Belda R, Megias R, Feito N, Vercher-Martinez A. Some practical considerations for compression failure characterization of open-cell polyurethane foams using digital image correlation. Sensors 2020;20:4141.
[4] Hoffmeister BK, Huber MT, Viano AM. Characterization of a polymer, open-cell rigid foam that simulates the ultrasonic properties of cancellous bone. J Acoust Soc Am 2018;(2):911–20. Feb; 143.
[5] Thompson MS, McCarthy ID, Lidgren L, Ryd L. Compressive and shear properties of commercially available polyurethane foams. J Biomech Eng 2003;125(5):732–4.
[6] Sawbones Catalogue. Available online: https://www.sawbone.com/catalog/biomechanical/blocks-and-sheets.html.
[7] Patel P, Shepherd D, Hukins D. Compressive properties of commercially available polyurethane foams as mechanical models for osteoporotic human cancellous bone. BMC Musculoskelet 2008;9:137.
[8] Kohli N, Stoddart JC, van Arkel RJ. The limit of tolerable micromotion for implant osseointegration: a systematic review. Sci Rep 2021;11(1):10797.
[9] Grupp TM, Schilling C, Schwiesau J, Pfaff A, Altermann B, Mihalko WM. Tibial implant fixation behavior in total knee arthroplasty: a study with five different bone cements. J Arthroplasty 2020;35:579–87.
[10] Nagel K, Bishop NE, Schlegel UJ, Püschel K, Morlock MM. The influence of cement morphology parameters on the strength of the cement-bone interface in tibial tray fixation. J Arthroplasty 2017;32:563–9.
[11] Pittmann GT, Peters CL, Hines JL, Bachus KN. Mechanical bond strength of the cement-tibial component interface in total knee arthroplasty. J Arthroplasty 2006;21:883–8.
[12] Lucchinetti. Review micromechanical testing of bone trabeculae - potentials and limitations. J Mater Sci 2000;35(24).
[13] Bini. Microtensile measurements of single trabeculae stiffness in human femur. J Biomech 2002;35(11).
[14] Thompson MS, Flivik G, Juliusson R, Odgaard A, Ryd L. A comparison of structural and mechanical properties in cancellous bone from the femoral head and acetabulum. Proc Inst Mech Eng H 2004;218(6):425–9.
[15] A Müller F, Fonseca Ulloa CA, Rickert M, Werner BS, Gohlke F. Press-fit reverse shoulder arthroplasty in case of advanced humeral bone loss - is additional distal fixation necessary for primary stability? Clin Biomech (Bristol, Avon) 2021;82:105283.
[16] Ahmed GA, Auge L, Loke J, Fonseca Ulloa CA, Fölsch C, Rickert M, Ishaque BA, Jahnke A. How screw connections influence the primary stability of acetabular cups under consideration of different bone models. J Orthop 2020;21:302–8.
[17] Gebert de Uhlenbrock A, Püschel V, Püschel K, Morlock MM, Bishop NE. Influence of time in-situ and implant type fixation strength of cemented tibila trays - a post mortem retrieval analysis. Clin Biomech 2012;27:929–35.
[18] Schlegel UJ, Siewe J, Delank KS, Eysel P, Püschel K, Morlock MM, Gebert de Uhlenbrock A. Pulsed lavage improves fixation strength of cemented tibial components. Int Orthop 2011;35:1165–9.
[19] Small SR, Rogge RD, Malinzak RA, Reyes EM, Cook PL, Farley KA, Ritter MA. Micromotion at the tibial plateau in primary and revision total knee arthroplasty: fixed versus rotating platform designs. Bone Joint Res 2016;5:122–9.
[20] Bhimji S, Meneghini M. Micromotion of cementless tibial baseplates: keels with adjuvant pegs offer more stability than pegs alone. J Arthroplasty 2014;29:1503–6.
[21] Luring C, Perlick L, Trepte C, Linhardt O, Perlick C, Plitz W, Grifka J. Micromotion in cemented rotating platform total knee arthroplasty: cemented tibial stem versus hybrid fixation. Arch Orthop Trauma Surg 2006;126:45–8.
[22] Han S, Patel RV, Ismaily SK, Jones HL, Gold JE. Micromotion and migration of cementless tibial trays under functional loading conditions. J Arthroplasty 2021;36(1):349–55.
[23] Miller MA, Terbush MJ, Goodheart JR, Izant TH, Mann KA. Increased initial cement-bone interlock correlates with reduced total knee arthroplasty micromotion following in vivo service. J Biomech 2014;47:2460–6.

[24] Miller MA, Goodheart JR, Izant TH, Rimnac CM, Cleary RJ, Mann KA. Loss of cement-bone interlock in retrieved tibial components from total knee arthroplasties. Clin Orthop Relat Res 2014;472:304–13.
[25] Peters CL, Craig MA, Mohr RA, Bachus KN. Tibial component fixation with cement. Clin Orthop Relat Res 2003;409:158–68.
[26] Sala M, Taylor M, Tanner KE. Torsional stability of primary total knee replacement tibial prostheses: a biomechanical study in cadaveric bone. J Arthroplasty 1999;14 (5):610–5.
[27] Chong DYR, Hansen UN, Amis AA. Analysis of bone-prosthesis interface micromotion for cementless tibial prosthesis fixation and the influence of loading conditions. J Biomech 2010;43:1074–80.
[28] Crook PD, Owen JR, Hess SR, Al-Humadi SM, Wayne JS, Jiranek WA. Initial stability of cemented vs cementless tibial components under cyclic load. J Arthroplasty 2017;32:2556–62.
[29] Lewis G. Properties of acrylic bone cement: state of the art review. J Biomed Mater Res 1997;38:155–82.